International Journal of Pure and Applied Physics. ISSN 0973-1776 Volume 13, Number 1 (2017), pp. 188-190


# Measurements of the L X-ray production cross sections for $_{74}$W at incident photon energies 12.1-13.0 keV using synchrotron radiation

**Rajnish Kaur, Anil Kumar, M.K. Tiwari* and Sanjiv Puri#**

#-Department of Basic and Applied Sciences, Punjabi University, Patiala-147002, Punjab, India

*- Synchrotron Utilization and Materials Research Division, RRCAT, Indore- 452013, India.

***Abstract*— The X-ray production cross sections for the $L_k$ (k=l, η, α, $\beta_{1,3,4,6}$, $\beta_{2,5,7,9,10,15}$, $\gamma_{1,5}$, $\gamma_{2,3,6,8}$) X-rays have been measured at five different incident photon energies ranging 12.1-13.0 keV for $_{74}$W using synchrotron radiation induced photoionization method in order to check the reliability of the IPA models at these incident photon energies. The measured values have been compared with two sets of theoretical values calculated using the non-relativistic Hartree-Fock-Slater (HFS) model based photoionization cross sections [6] tabulated by Scofield (1973), Dirac-Fock (DF) model based X-ray emission rates [7] provided by Campbell and Wang (1989), fluorescence ($\omega_i$) and Coster-Kronig ($f_{ij}$) yields [8] recommended by Campbell (2003, 2009) and the Dirac-Hartree-Slater (DHS) model based yield values [9] tabulated by Puri et al (1993). The present measured $L_k$ (=l, η, α, $\beta_{1,3,4,6}$, $\beta_{2,5,7,9,10,15}$, $\gamma_{1,5}$, $\gamma_{2,3,6,8}$) X-ray production (XRP) cross sections exhibited significant differences with both the calculated set values.**

***Index Terms*— Synchrotron radiation, X-ray production cross sections.**

## I. INTRODUCTION

The measurements of X-ray production (XRP) cross sections are important for a variety of applications in the field of atomic and radiation physics including radiation shielding, radiation dosimetry, medical diagnosis and therapy, and elemental composition analysis using X-ray emission techniques (EDXRF and PIXE). The XRP cross sections can be evaluated from the physical parameters, namely, the X-ray emission rates, the photoionization cross sections, fluorescence and Coster-Kronig (CK) yields. A number of reports on the experimental investigations of the photon induced L-shell X-ray production cross sections are available in literature. Most of these reports pertains to measurements of the $L_i$ (i=1-3) sub-shell X-ray production cross sections at incident photon energies much above the $L_i$ (i=1-3) sub-shell absorption edge energies [2]-[5] performed to test the reliability of the IPA models [1]. However, to the best of our knowledge, similar investigations at incident photon energies in vicinity of the $L_1$ sub-shell ionization threshold of heavy elements are not available in literature.

In the present work, the cross sections for production of the $L_k$ (k=l, η, α, $\beta_{1,3,4,6}$, $\beta_{2,5,7,9,10,15}$, $\gamma_{1,5}$, $\gamma_{2,3,6,8}$) X-rays have been measured at five incident photon energies ranging 12.1-13.0 keV, just above the $L_1$ sub-shell ionization threshold of $_{74}$W employing synchrotron radiation induced photoionization method. The measured values have been compared with two sets of theoretical values calculated using the non-relativistic Hartree-Fock-Slater (HFS) model based photoionization cross sections [6], the Dirac-Fock (DF) model based X-ray emission rates [7], the fluorescence ($\omega_i$) and Coster-Kronig(CK) ($f_{ij}$) yields recommended by Campbell [8] and those based on the Dirac-Hartree-Slater (DHS) model [9].

## II. EXPERIMENTAL DETAILS

The present measurements were performed using the micro-focus X-ray fluorescence beam-line (BL-16) of INDUS-2 synchrotron radiation facility. The salient features of beam-line BL-16 and details of the X-ray fluorescence (XRF) setup are described elsewhere [10]. The electron storage ring at INDUS-2 was operated at 2.53 GeV with a nominal current of 100 mA. A Si (111) double crystal monochromator (DCM) capable of tuning the photon energy in the range 4-15 keV with energy resolution ~$10^{-3}$-$10^{-4}$ was used to obtain a monochromatic photon beam of desired energy on the sample position. The size of the X-ray beam at the target position was controlled using JJ slit having size ~800 μm (H) × 200 μm (V). The target holder was placed at 45° with respect to the incident beam direction. The monochromatic beam was allowed to pass through an ionization chamber (aperture size: 10 mm×6 mm; FMB OXFORD, UK) before reaching the target in order to monitor the incident photon beam intensity ($I_0$). The Vortex-EX90 silicon drift detector (50 mm$^2$×350 μm, FWHM~140 eV at 5.89 keV, Be window thickness~1 mil, SII Nano Tech. Inc., USA) coupled to a digital pulse processor (XIA LLC, USA) was placed at 90° with respect to the incident beam direction to detect emitted X-rays.

Date of submission: 1 November, 2016

Rajnish Kaur, Anil Kumar, M. K. Tiwari* and Sanjiv Puri#

*# Department of Basic and Applied Sciences, Punjabi University, Patiala, Punjab, India-147002.*

**- Synchrotron Utilization and Materials Research Division, RRCAT, Indore-452013, India.*

*# e-mail:* sanjivpurichd@yahoo.com

# Corresponding author. E-mail: sanjivpurichd@yahoo.com; Ph: +91 175 3046323; FAX: +91 175 3046333

Spectroscopically, pure self-supporting $_{74}$W (metallic foil) having mass thickness 96 mg/cm$^2$ was used as the target. The L X-rays were excited using monochromatic X-ray beam by varying its energy in small steps over the range 12.1-13.0 keV just above the $L_1$ ionization threshold energy of $_{74}$W. Typical L X-ray spectrum for $_{74}$W recorded at the 13.0 keV incident photon energy is shown in Fig. 1.

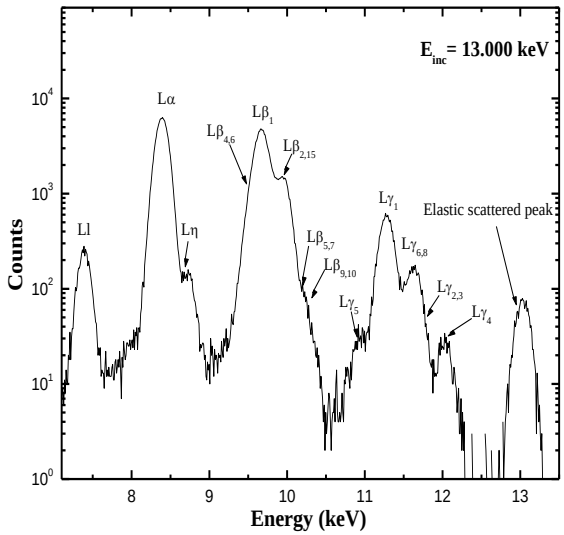


**Fig. 1:** A typical spectrum of $_{74}$W target at 13.000 keV incident photon energy depicting the $L_1$, $L_2$ and $L_3$ sub-shell fluorescent X-rays.

## III. EVALUATION PROCEDURE

The experimental $L_k$ (k= l, α, η, $\beta_{2,5,6,7,15}$, $\beta_{1,6}$, $\beta_{1,3,4,6}$, $\gamma_{1,5}$, $\gamma_{2,3,6,8}$) X-ray production (XRP) cross sections, $\sigma_{Lk}(exp)$, at different incident photon energies ($E_{inc}$) have been evaluated using the relation

$$\sigma_{Lk}(exp) = N_{Lk}/(I_0 G\varepsilon_{Lk}\,\beta_{Lk} m)$$

where $N_{Lk}$ represents the counts under the $L_k$ photo-peak, $I_0G$ is the incident photon intensity falling on the area of the target visible to the detector, $\varepsilon$ is the detector efficiency at the $L_k$ X-ray energy, $m$ is the mass thickness (gm/cm$^2$) of the target and $\beta_{Lk}$ is the self-absorption correction factor which accounts for the absorption of incident and emitted photons in the target.

The values of self-absorption correction factor ($\beta_{Lk}$) have been evaluated as explained in our earlier reference [2]. In these evaluations, the values of mass-attenuation coefficients for the incident and emitted X-rays were taken from the computer code XCOM [11]. Each spectrum was analyzed for peak areas, $N_{Lk}$, using software package ORIGIN 6.0 in which a non-linear least squares fitting routine based on chi-square minimization using Marquardt's algorithm [12] has been implemented. The peak fitting for different L X-ray spectra were performed as explained in our earlier references [2, 4, 5, 13]. The product $G\varepsilon$ was determined as explained in our earlier reference [13] by measuring the K X-ray yields excited by 13 keV incident photons from self-supporting thick pressed pellets (1 inch diameter) of ZnS, $GeO_2$, Se, $As_2O_3$ and metallic foils of Ti, Co, Fe, Ni, Cu in the same geometrical set up. In these evaluations, the theoretical values of the K X-ray production (XRP) cross sections, $\sigma^{x}_{K\alpha}$, were taken from reference [14].

The current status of different $L_i$ (i=1-3) sub-shell physical parameters, namely, the photoionization cross sections, X-ray emission rates, fluorescence and CK yields, required to evaluate XRP cross sections / intensity ratios has been discussed in our earlier reference [15]. In the present work, two sets of the theoretical $L_k$ (k= l, η, α, $\beta_{1,3,4,6}$, $\beta_{2,5,7,9,10,15}$, $\gamma_{1,5}$, $\gamma_{2,3,6,8}$) XRP cross sections, $\sigma_{Lk}$(Camp.) and $\sigma_{Lk}$(DHS), respectively, have been calculated using the non-relativistic Hartree-Fock-Slater (HFS) model based photoionization cross sections [6], the Dirac-Fock (DF) model based X-ray emission rates [7], the fluorescence ($\omega_i$) and Coster-Kronig ($f_{ij}$) yields recommended by Campbell [8] and those based on the Dirac-Hartree-Slater (DHS) model [9].

## IV. RESULTS AND DISCUSSIONS

The present measured $L_k$ (k= l, α, η, $\beta_{2,5,6,7,15}$, $\beta_{1,6}$, $\beta_{1,3,4,6}$, $\gamma_{1,5}$, $\gamma_{2,3,6,8}$) XRP cross sections, $\sigma_{Lk}$(exp), have been compared with two sets of calculated values, $\sigma_{Lk}$(Camp.) and $\sigma_{Lk}$(DHS), by plotting the ratios [$\sigma_{Lk}$(exp)/ $\sigma_{Lk}$(Thr.)] as a function of incident photon energies in Figs. 2-4. The overall error in the present measured cross sections is estimated to be 6-9% and is obtained as quadrature sum of the uncertainties in different parameters used to evaluate these cross sections, namely , the evaluation of photo peak areas (1-4%), $I_oG\varepsilon$ product (~5-7%), target thickness (< 2%) and in the absorption correction factor (<4%).

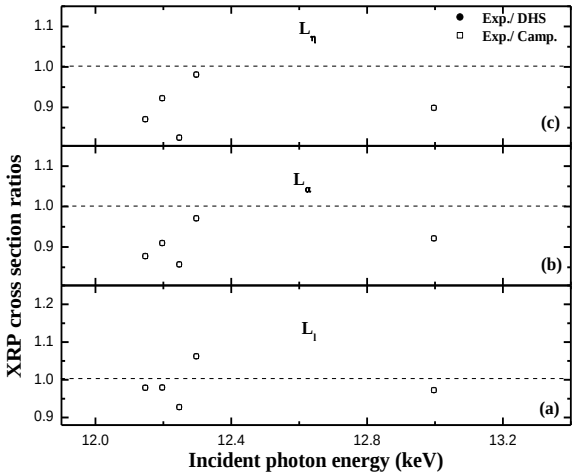


**Fig. 2:** A plot of ratios of the present measured (a) the Ll (b) the Lα (c) the Lη XRP cross sections to the two sets of calculated values [$\sigma_{Lk}$(DHS) and $\sigma_{Lk}$(Camp.); k = l, α, η] for $_{74}$W as a function of incident photon energy.

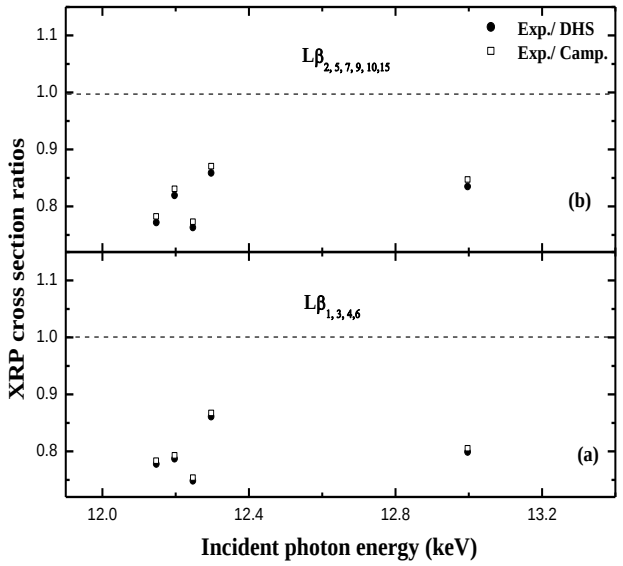


**Fig. 3:** A plot of ratios of the present measured (a) $L\beta_{1,3,4,6}$ (b) $L\beta_{2,5,7,9,10,15}$ XRP cross sections to the two sets of calculated values [$\sigma_{Lk}$(DHS) and $\sigma_{Lk}$(Camp.); k = $\beta_{1,3,4,6}$ , $\beta_{2,5,7,9,10,15}$ ] for $_{74}$W as a function of incident photon energy.

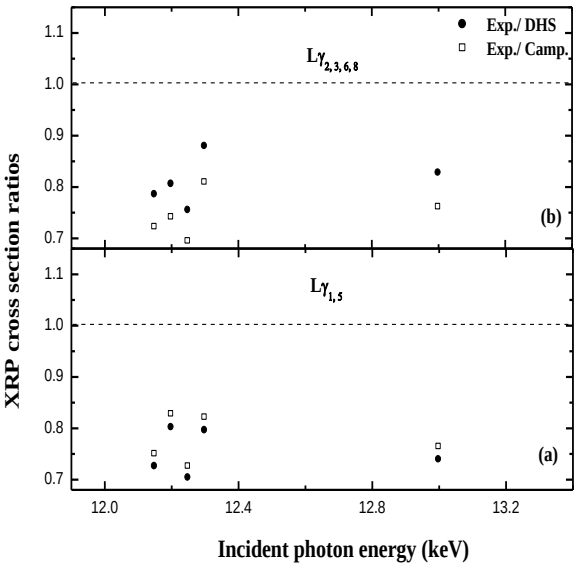


**Fig 4:** A plot of ratios of the present measured (a) the $L\gamma_{1,5}$ (b) the $L\gamma_{2,3,6,8}$ XRP cross sections to the two sets of calculated values [$\sigma_{Lk}$(DHS) and $\sigma_{Lk}$(Camp.); k= $\gamma_{1,5}$, $\gamma_{2,3,6,8}$ ] for $_{74}$W as a function of incident photon energy.

The $\sigma_{Lk}$(DHS) values are found to be higher than $\sigma_{Lk}$(Camp.) values by up to 3% for the $L_2$ and the $L_3$ sub-shell X-rays (l, α, η , $\beta_{1,6}$, $\beta_{2,15,5,7}$, $\gamma_{1,5}$, $\gamma_{6,8}$) and lower by up to 10% for $L_1$ sub-shell X-rays (k= $\beta_{3,4}$, $\gamma_{2,3}$ ). These differences are due to differences in the $L_1$ sub-shell fluorescence and CK yields ($\omega_1$, $f_{12}$ and $f_{13}$) recommended by Campbell [8] and those based on the DHS model [9]. The present measured cross sections, $\sigma_{Lk}$(exp) (k= l, α, η, $\beta_{2,5,6,7,15}$, $\beta_{1,6}$, $\beta_{1,3,4,6}$, $\gamma_{1,5}$, $\gamma_{2,3,6,8}$), are found to be lower by up to 25% than two sets of calculated values (Figs. 2-4).

ACKNOWLEDGMENT

The authors acknowledge the technical assistance provided by Mr. Ajit singh during the beam time at the XRF beam line of INDUS-II, RRCAT, Indore.

## REFERENCES

[1] B. Crasemann," *Atomic Inner-Shell Processes*," Part A, Academic Press, New York, 1985.

[2] S. Puri, D. Mehta, N. Singh, P.N. Trehan, "The $L\gamma_{1,5}$ , $L\gamma_{2,3,6}$ , $L\gamma_4$, and Lα x-ray fluorescence cross sections for the elements with 71≤ Z ≤ 83 at 22.6 keV, " *Phys. Rev. A*, vol. 54, pp. 617, Jan. 1996.

[3] S. Puri, N. Singh," $L_i$ (i =1–3) subshell fluorescence and Coster-Kronig yields for elements with 70 ≤ Z ≤ 92," *Radiat. Phys. Chem.*, vol. 75, pp. 2232, March 2006 and references therein.

[4] Y. Chauhan, M. K. Tiwari and S. Puri," $L_i$ (i = 1–3) subshell X-ray production cross sections and fluorescence yields for some elements with 56 ≤ Z ≤ 68 at 22.6 keV," *Nucl. Instrum. and Methd. B*, vol. 266, pp. 30, Oct. 2008.

[5] A. Kumar and S. Puri," $L_1$ and $L_2$ sub-shell fluorescence yields for elements with 64 ≤ Z ≤ 70," *Nucl. Instrum. and Methd. B,* vol. 268, pp. 1546, Feb. 2010.

[6] J. H. Scofield," Theoretical Photoionization Cross Sections from 1 to 1500 keV," *Lawrence Livermore Laboratory (UCRL)*, Report 51326, 1973.

[7] J.L. Campbell and J.X. Wang," Interpolated Dirac–Fock values of L sub-shell X-ray emission rates including overlap and exchange effects," *At. Data Nucl. Data Tables*, vol. 43, pp. 281, 1989.

[8] J.L. Campbell," Fluorescence yields and Coster–Kronig probabilities for the atomic L subshells," *At. Data Nucl. Data Tables*, vol. 85, pp, 291, 2003; "Fluorescence yields and Coster–Kronig probabilities for the atomic L subshells. Part II:The L1 sub-shell revisited," *At. Data Nucl. Data Tables*, vol. 95, pp. 115, 2009.

[9] S. Puri, D. Mehta, B. Chand, N. Singh, P. N. Trehan," L Shell Fluorescence Yields and Coster-Kronig Transition Probabilities for the Elements with *25≤ Z ≤ 96*," *X-Ray Spectrom.*, vol. 22, pp. 358, 1993.

[10] M. K. Tiwari, P. Gupta, A. K. Sinha, C. K. Garg, A. K. Singh, S. R. Kane, S. R. Garg and G. S. Lodha,"Commissioning of a microprobe-XRF beamline (BL-16) on Indus-2 synchrotron source," in Proc. AIP Conference 1447, 2012, pp. 499; doi: 10.1063/1.4710097. Available online: http://www.cat.gov.in/technology/accel/srul/beamlines/xrf.html

[11] M.J. Berger, J.H. Hubbell, S.M. Seltzer, J. Chang, J.S. Coursey, R. Sukumar, D.S., Zucker and K. Olsen," *XCOM: Photon Cross Section Database (web version 1.5)*," National Institute of Standards and Technology, Gaithersburg, MD, 2010. Available online: http://physics.nist.gov/xcom

[12] P. R. Bevington, "*Data Reduction and Error Analysis for Physical Sciences*, McGraw-Hill, New York, 1969.

[13] A. Kumar and S. Puri," Chemical effects on the $L_i$ (i=1–3) sub-shell X-ray relative intensities for some compounds of Hg," *Radiation Physics and Chemistry*, vol. 80, pp. 1166, May 2011.

[14] S. Puri, B. Chand, D. Mehta, M.L. Garg, N. Singh and P.N. Trehan," K and L shell X-ray fluorescence cross sections," *At. Data Nucl. Data Tables*, vol. 61, pp. 289, 1995.

[15] S. Puri," Physical parameters for atomic inner-shell photoionization processes and analytical applications: a status report," *X-ray Spectrom.*, vol. 40, pp. 348, July 2011.